SMJ- Sohag Medical Journal, Vol. 28 No (2) 2025

Print ISSN1687-8353 Online ISSN2682-4159

Original Article

Role of diagnostic imaging in evaluation of cochlear implant candidate

Marwa Helmy Elhadad[1], Mohammad Tharwat Solyman[1], Ramadan Hashem Sayed[2], Mohamad Alam-Eldeen[1],

1-Department of Diagnostic Radiology - Faculty of Medicine - Sohag University
2-Department of Otorhinolaryngology, Faculty of Medicine, Sohag University, Egypt

Abstract

Background: Preoperative imaging evaluation is crucial for successful cochlear implantation (CI). This study aimed to systematically identify congenital and acquired inner ear abnormalities, evaluate cochlear nerve anomalies, and detect temporal bone variations requiring surgical modifications during CI.

Methods: A prospective study was conducted on 100 CI candidates with severe to profound sensorineural hearing loss at our hospital, during 2024. All patients underwent high-resolution MSCT and MRI. Cochlear parameters, including duct length and height, were measured using software-based methods.

Results: The radiological assessment revealed identical findings between CT and MRI for cochlear development, with 85% showing well-developed structures and 15% presenting maldevelopment. Among malformed cases, incomplete partition type II was most prevalent (46.67%). Cochlear patency evaluation showed a patent cochlea in 97% of cases. The mean cochlear duct length was approximately 31.2mm bilaterally. MRI evaluation of the cochlear nerve demonstrated normal morphology in 95% of cases. The internal auditory canal was normal in 99% of cases, while the vestibular aqueduct was normal in 86%, dilated in 13%, and absent bilaterally in 1% of cases. Both imaging modalities showed consistent findings across all measured parameters, with superior MRI regarding cochlear nerve evaluation.

Conclusions: Combined CT and MRI provide complementary information crucial for preoperative evaluation of CI candidates, enabling detailed assessment of temporal bone anatomy, inner ear malformations, and neural integrity, essential for optimal surgical planning and outcome prediction.

sensorineural hearing loss (SNHL), cochlear implant (CI), internal auditory canal (IAC), cochlear duct length (CDL).

Keywords: Cochlear implant, CT, MRI, temporal bone, inner ear malformations

Abbreviations: incomplete partition (IP), Semicircular canal (SCC), vestibular aqueduct (VA),

DOI : 10.21608/SMJ.2025.389245.1577 **Received:** May 08 , 2025 **Accepted:** June 08 , 2025

Published: June 18, 2025

Corresponding Author: **Marwa Helmy Elhadad** **E.mail**: marwahelmy2481986@gmail.com

Citation: **Marwa Helmy Elhadad. et al.,** Role of diagnostic imaging in evaluation of cochlear implant candidate **SMJ,**2025 Vol. 29 No (2) 2025 116- 125

Introduction:

The temporal bone, situated at the skull base, comprises the squamous, petrous, mastoid, and tympanic parts, along with the styloid process, crucial for auditory and vestibular functions. [1,2] It houses vital structures like the cochlea, vestibule, semicircular canals, and facial nerve, with the cochlea converting sound into neural signals [3,4]. Its development involves endochondral and membranous ossification.[2] Congenital anomalies, such as labyrinthine aplasia and incomplete partition (IP) types I-III, disrupt hearing and balance. [5,6]. Semicircular canal (SCC) and vestibular aqueduct (VA) anomalies further impair these functions. [7,8] Acquired disorders like labyrinthitis ossificans and perilymphatic fistulas complicate surgical interventions.[9]

Cochlear implantation provides transformative treatment for severe sensorineural hearing loss (SNHL), directly stimulating the auditory nerve when cochlear structures fail. [10,11] Successful outcomes depend on accurate electrode placement in the scala tympani, guided by understanding cochlear anatomy, particularly the basal turn and round window. [12,13]

Both CT and MRI are complementary imaging modalities that enable the detection of cochlear and middle ear anatomy, as well as anatomical variations. [8,14]

CT imaging is crucial for evaluating cochlear implant (CI) candidates, offering high-resolution visualization of the bony structures of the temporal bone, including the cochlea, vestibule, SCCs, and internal auditory canal (IAC). [15,16] Axial, coronal, and sagittal sections provide detailed views of key structures like the facial nerve canal, carotid canal, ossicles, and jugular foramen. [17] CT identifies congenital anomalies, such as cochlear hypoplasia or enlarged VA, and acquired conditions like labyrinthitis ossificans, which influence surgical planning, electrode selection, and technique adjustments. [18]

MRI, with its superior soft tissue contrast, complements CT in evaluating CI candidates by visualizing the cochlear nerve and membranous labyrinth. High-resolution T2-weighted sequences effectively assess the fluid-filled inner ear spaces and IAC, revealing the cochlea's internal architecture, interscalar septa, modiolus, and the course of the vestibulocochlear and facial nerves. [8] MRI detects conditions like labyrinthitis ossificans, cochlear nerve aplasia, and soft tissue lesions, such as vestibular schwannomas or meningiomas, that influence candidacy and surgical planning. [19]

This study aimed to systematically identify congenital and acquired abnormalities of the inner ear, evaluate anomalies of the cochlear nerve, and detect temporal bone abnormalities necessitating surgical modifications during cochlear implantation.

Patients and Methods:

A prospective study was conducted 100 patients with clinically diagnosed severe to profound SNHL who met the CI criteria at our hospital during 2024.

The study protocol received approval from the Ethics Committee of our Faculty, and informed consent was obtained from all participants. Patients of any age and gender who fulfilled the audiological and phoniatric criteria for CI were included, while those who did not meet these criteria were excluded.

Preoperative imaging assessments were performed using both CT and MRI.

CT examinations were conducted using a Toshiba Alexion 16-slice scanner, with unenhanced 0.6 mm axial slices obtained in the neutral supine position. The axial source images were processed using a dedicated workstation to generate coronal and sagittal oblique multiplanar reformatted images of the cochlea and SCCs bilaterally. Scans were acquired through the temporal bone using a 512 × 512 matrix, extending from the petrous apex to the mastoid tip. Images were displayed at a window centering level of 700 HU and a window width of 4000 HU.

Cochlear parameters were measured using software-based methods, including length estimation based on the A-value method. The cochlear duct length (CDL) was calculated using Alexiades' equation: CDL = (4.16 × A - 4), where the A-value represented the straight line from the round window membrane midpoint to the opposite cochlear side through the mid-modiolar axis. Additional measurements included cochlear height, round window accessibility, IAC dimensions, and temporal bone cortical thickness for transducer placement and screw fixation **(Figure 1)**.

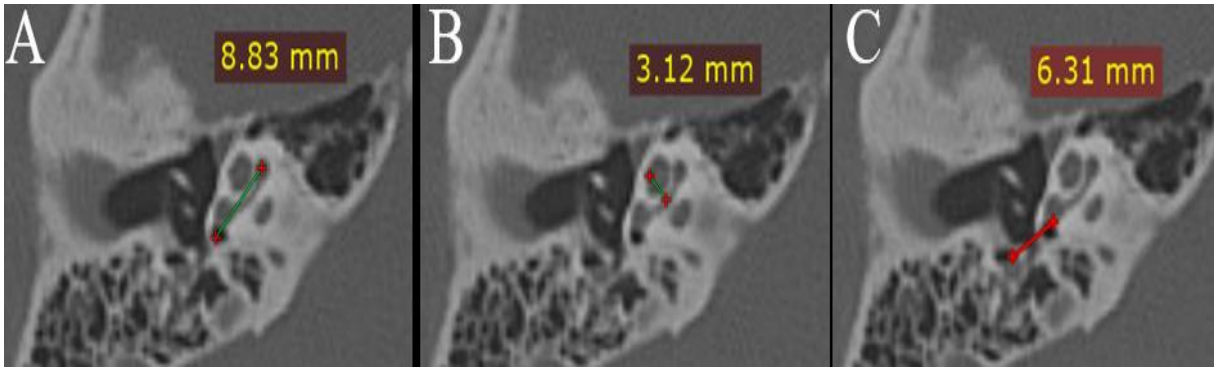

Figure.1: Axial images of a normal cochlea showing the used measures. (A) shows how to measure cochlear duct length, (B) shows how to measure cochlear duct height, (C) shows how to assess round window accessibility in relation to facial nerve position.

MRI examinations were performed using a 1.5T Philips Achieva system with a dedicated head coil. The protocol comprised axial and coronal B_TFE sense sequences of the inner ear, oblique sagittal T2W_3D_DRIVE CLEAR sequences of the IAC, and fluid-attenuated inversion recovery (FLAIR) images of the brain. Sequence parameters were optimized for detailed visualization of the cochlear nerve and central nervous system pathology. Light sedation was administered to children under six years and uncooperative patients to ensure image quality. None of our patients needed IV contrast administration.

Statistical analysis

Statistical analysis was done by SPSS v26 (IBM$^{Inc.}$, Chicago, IL, USA). Quantitative variables were presented as mean and standard deviation (SD). Qualitative variables were presented as frequency and percentage (%).

Results:

The study included 100 candidates with severe to profound SNHL with mean age 4 ± 2.77 years (Table 1).

Table 1: Demographic data of the studied patients

		n=100
Age (years)		4 ± 2.77
Sex	**Male**	54 (54%)
	Female	46 (46%)

Data are presented as mean±SD or frequancy (%).

Radiological assessment of cochlear development using both CT and MRI demonstrated identical findings, with 85% of patients exhibiting well-developed cochlear structures, while 15% presented with maldevelopment (Table 2).

Table 2: Cochlear development demonstrated by CT, MRI of the studied patients

	CT (n=100)	MRI (n=100)
Well developed	85 (85%)	85 (85%)
Maldeveloped	15 (15%)	15 (15%)

Data are presented as frequancy (%).

Among maldeveloped cases, IP type 2 was predominant (46.67%) **(Figure 2)**. Other anomalies included IP type 1 (13.33%) **(Figure 3)**, dysplasia (6.67%), unilateral complete aplasia (6.67%) **(Fig.4)**, vestibulo-cochlear malformation (6.67%), and labrynthitis ossificans (20%) **(Fig.5)**
(Table 3).

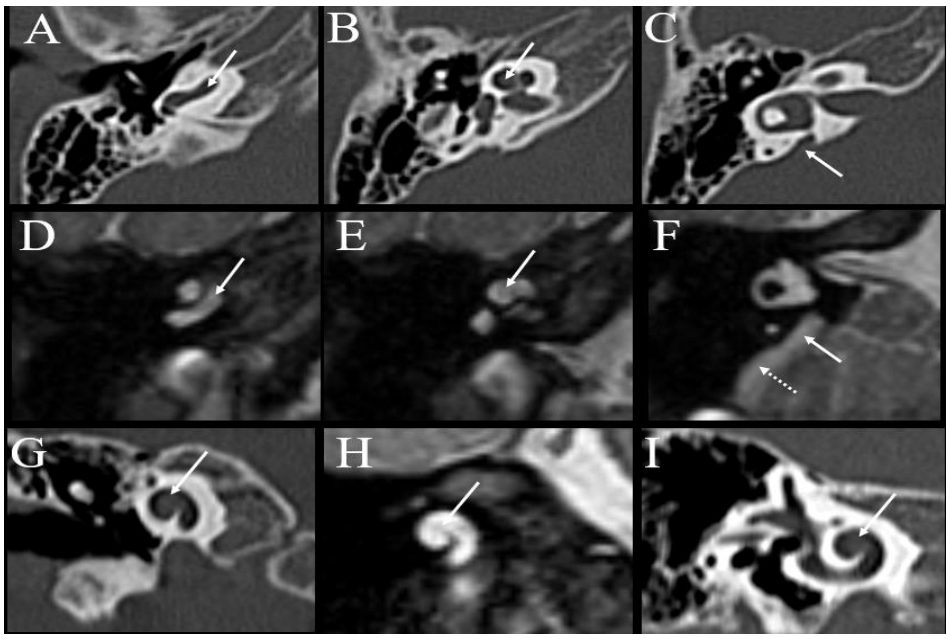

Fig.2: Patient 5 years old with right incomplete partition type 2. (A,D) Axial CT and MRI showing normal cochlea basal turn (arrows). (B,E) Axial CT and MRI showing cystic configuration of cochlea apical and middle turns with abscent interscalar septum (arrows). (C,F) Axial CT and MRI showing dilated endolymphatic duct on CT (arrow) and dilated endolymphatic duct (arrow) and endolymphatic sac (dashed arrow) on MRI, (G,H) Coronal CT and MRI showing cystic configuration of cochlea apical and middle turns with abscent interscalar septum (arrows). (I) Sagittal oblique MPR CT image showing the whole cochea and confirmed cystic configuration of apical and middle turns.

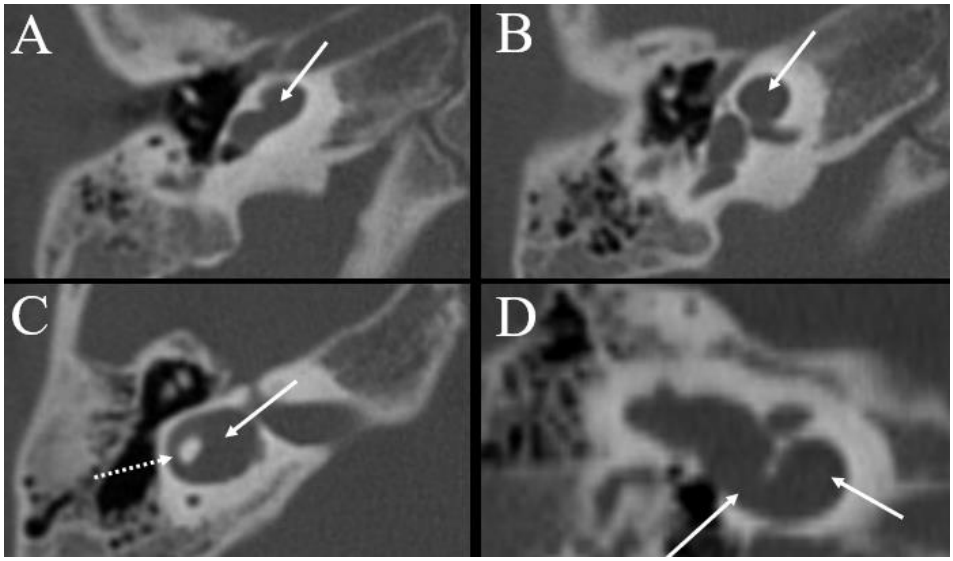

Fig.3: Patient 4 years old with right incomplete partition type 1. (A,B,C) Serial axial CT images showing wide cochlea basal turn (arrow on A), markedly dilated middle and apical turns with cystic configuration (arrow on B), dilated vestibule (solid white arrow on C) with short hypoplastic lateral SCC (dashed white arrow on C). (D) Sagittal oblique MPR CT image showing dilated whole cochlea with cystic configuration.

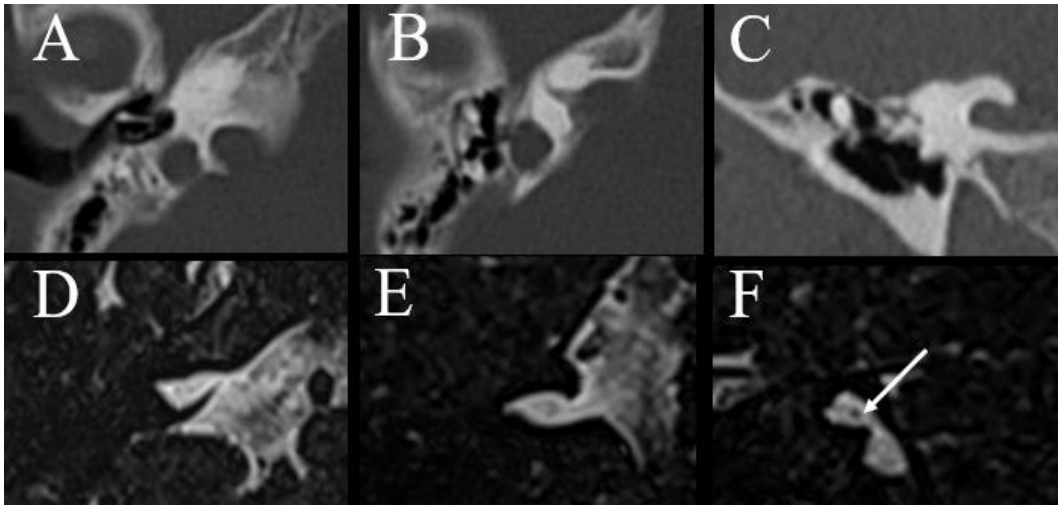

Figure 4: Patient 2 years old with right inner ear aplasia. (A,B) Axial and (C) coronal CT images showing complete abscence of inner ear structures. (D,E) Axial MRI showing same findings. (F) Sagittal oblique MRI on right IAC showing only the facial nerve (arrow) with abscent vestibulo-cochlear bundle.

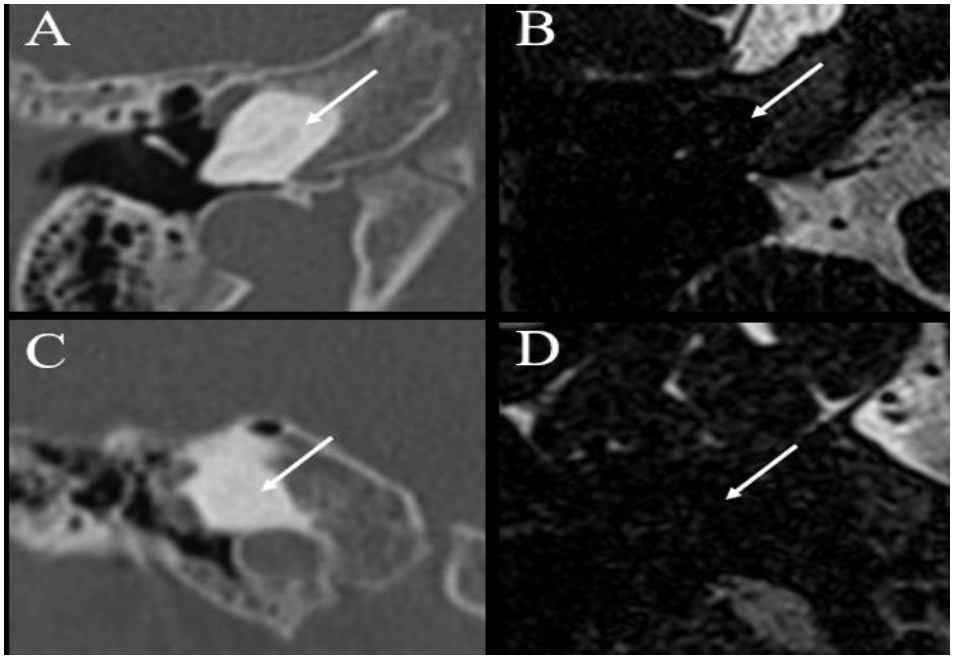

Figure 5: Patient 3 years old with labyrinthitis ossificans of right cochlea. (A,B) Axial CT and MRI showing complete ossification of cochlea lumen (arrows). (C,D) Coronal CT and MRI showing same findings (arrows).

Table 3: Cochlear anomalies by CT and MRI of the studied patients

(n=15)	CT	MRI
Dysplasia	1 (6.67%)	1 (6.67%)
Incomplete partition Type 1	2 (13.33%)	2 (13.33%)
Incomplete partition Type 2	7 (46.67%)	7 (46.67%)
RT complete aplasia-LT dysplastic	1 (6.67%)	1 (6.67%)
RT cystic vestibulo- cochlear malformation -LT normal	1 (6.67%)	1 (6.67%)
RT well developed - LT labrynthitis ossificans	3 (20%)	3 (20%)

Data are presented as frequancy (%).RT:Right, LT: Left.

Cochlear patency evaluation revealed 97% patent cases and 3% partially ossified. Vestibule/SCC assessment showed 94% patent structures, with remaining cases displaying various anomalies including bilateral absent lateral SCC (1%), partial ossification (3%), and unilateral dysplasia (1%) (Table 4).

Table 4: Cochlear patency by CT and Vestibule / semicircular canals by CT and MRI of the studied patients

Cochlear patency by CT	n=100	
Patent	97 (97%)	
Not patent (Partially ossified)	3 (3%)	
Vestibule / semicircular canals by CT and MRI		
	CT (n=100**)**	**MRI (**n=100**)**
Patent	94 (94%)	94 (94%)
Bilateral absent lateral SCC	1 (1%)	1 (1%)
Partially ossified	3 (3%)	3 (3%)
RT dysplastic, LT normal	1 (1%)	1 (1%)
Absent	1 (1%)	1 (1%)

Data are presented as frequancy (%). RT:Right, LT: Left. SCC: Semicircular Canals.

The mean cochlear duct length was 31.2 ± 2.27mm (right) and 31.3 ± 2.46mm (left), while mean duct height was 3.4 ± 0.36mm (right) and 3.4 ± 0.38mm (left) **(Fig.6 A,B)** (Table 5).

Table 5: Cochlear duct length and height measured in CT of the studied patients

	n=100
RT cochlear duct length (mm)	31.2 ± 2.27
LT cochlear duct length (mm)	31.3 ± 2.46
RT cochlear duct height (mm)	3.4 ± 0.36
LT cochlear duct height (mm)	3.4 ± 0.38

Data are presented as mean±SD. RT:Right, LT: Left.

Mastoid pneumatization analysis revealed predominantly pneumatic cells (81%), followed by mixed (12%), sclerotic (4%), and diploic (3%) patterns. Facial nerve showed typical posterior course in 97% of cases **(Fig.6 C)**. Round window accessibility was radiologically favorable in 97% of patients (Table 6).

Table 6: Mastoid air cells, facial nerve location and round window accessibility by CT of the studied patients

		n=100
Mastoid air cells	**Penumatic**	81 (81%)
	Diploic	3 (3%)
	Sclerotic	4 (4%)
	Mixed	12 (12%)
Facial nerve location	**Anterior**	3 (3%)
	Posterior	97 (97%)
Round window accessibility	**Easy**	97 (97%)
	Difficult	3 (3%)

Data are presented as frequancy (%).

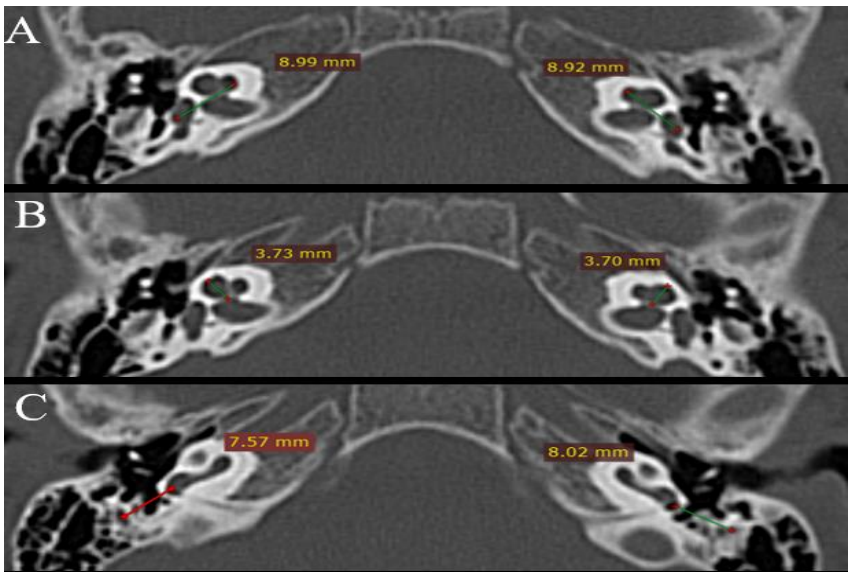

Figure 6: Serial axial CT images showing bilateral measurements of cochlear duct length and height and assessment of the position of facial nerve in relation to the round window.

MRI evaluation of the cochlear nerve revealed normal morphology in 95% of cases. Bilateral absence was observed in 2%, unilateral absence in 2%, and unilateral hypoplasia in 1% of patients **(Figure.7)** (Table 7).

Table 7: Cochlear nerve by MRI of the studied patients

	n=100
Normal	95 (95%)
Bilateral absent	2 (2%)
RT absent / LT normal	2 (2%)
RT hypoplasia / LT normal	1 (1%)

Data are presented as frequancy (%).RT:Right, LT: Left.

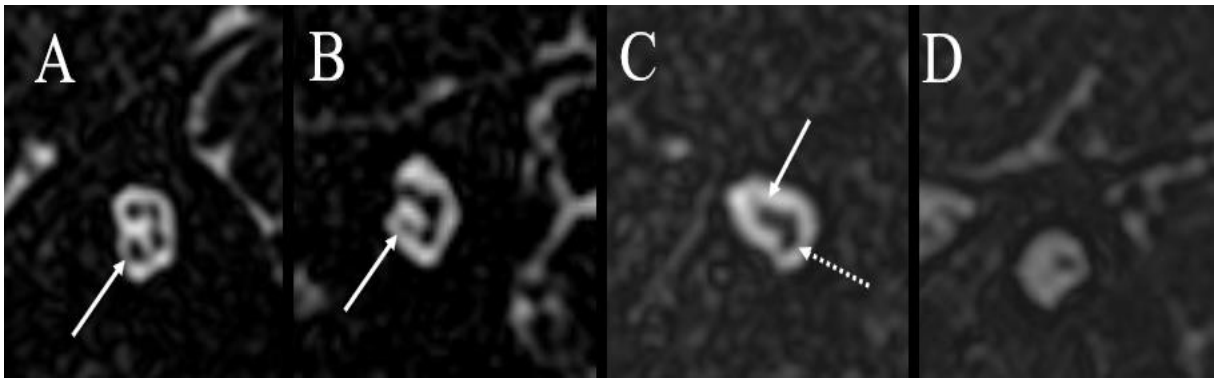

Figure 7: Sagittal oblique MRI on IAC in four different patients. (A) Normal cochlear nerve (arrow). (B) Hypoplastic cochlear nerve (arrow). (C) Normal facial nerve (solid white arrow) and normal vestibular nerve (dashed white arrow) with abscent cochlear nerve. (D) Only the facial nerve is seen with abscent vestibulo-cochlear bundle.

CT findings showed normal cochlear aqueduct in 99% and normal vestibular aqueduct in 86% of cases. Mean temporal bone thickness was 7.3 ± 0.77mm. Middle ear abnormalities were present in 22% of cases. Incidental mild brain atrophic changes were noted in 6% (Table 8).

Table 8: Cochlear aqueduct, Vestibular aqueduct, cortical thickness of temporal bone at the site of internal device, external auditory canal, middle ear and other occasionally detected findings by CT of the studied patients

		n=100
Cochlear aqueduct	Normal	99 (99%)
	Bilateral absent	1 (1%)
Vestibular aqueduct	Normal	86 (86%)
	Bilateral absent	1 (1%)
	Dilated	13 (13%)
Temporal bone thickness (mm)	7.3 ± 0.77	
External auditory canal	Normal	100 (100%)
Middle ear	Normal	78 (78%)
	Bilateral soft tissue opacity	21 (21%)
	RT soft tissue opacity/ LT normal	1 (1%)
Others	No abnormality	94 (94%)
	Mild brain atrophic changes	6 (6%)

Data are presented as mean±SD or frequancy (%).RT:Right, LT: Left.

The IAC canal was normal in 99% of cases.

Discussion:

Hearing impairment is the most common sensory deficit in children, significantly affecting development, particularly when occurring postnatally or in infancy. [20] CI is a critical intervention for severe-to-profound SNHL, especially when hearing aids provide limited benefit. [21] A thorough understanding of cochlear anatomy and its variations is vital for implant surgeons and radiologists due to increasing CI utilization. [22]

CT imaging revealed well-developed cochleae in 85% of patients, with malformations observed in the remaining 15%. IP type II was the commonest anomaly detected in our series (7/15=46.67%) followed by labyrinthitis ossificans (3/15=20%). MRI confirmed these findings of cochlear development in the same way like CT,with the advantage of avoiding radiation exposure, particularly in pediatric patients. Both Parry et al. and Connor et al. reported this advantage of MRI over CT.[23,24] Similar findings of various cochlear anomalies, including IP and cochlear hypoplasia were reported by Dawoud et al. [25] and Wu et al. [26] in their respective cohorts.

Cochlear patency was observed in 97% of patients, with partial ossification noted in 3%, consistent with findings by Dawoud et al. [25] and Wu et al.[26]. However, Keidar et al. [27] reported a higher incidence of inner ear opacification (25%), potentially attributable to differences in the age distribution of their study population. Measurements of cochlear duct length and height were comparable in both CT and MRI, with mean values aligning closely with those reported by Dawoud et al. [25] and Swarup et al. [28]

Vestibular and SCC abnormalities were identified in 6% of patients, with MRI providing additional diagnostic value in detecting endolymphatic sac dilatation. Tiwari et al.[29] and Dawoud et al. [25] reported similar findings, although Abd Alla et al. [30] observed a higher prevalence of SCC dysplasia (10%). Mastoid pneumatization was predominantly pneumatic (81%), with sclerotic or mixed patterns observed in a minority of cases. Facial nerve positioning and round window accessibility were consistent with previous studies.[30] CT is more informative in this aspect due to MRI's limitations in visualizing the round window niche due to hyperintense fluid signals.

Cochlear and vestibular aqueduct abnormalities were rare, with bilateral absence of both observed in 1% of patients, and dilatation of the VA in 13%. These findings align with those of Tiwari et al. [29] and Dawoud et al. [25] although Abd Alla et al.[30] reported a higher incidence of VA dilatation (11.6%). Cochlear nerve assessment by MRI revealed bilateral absence in 2% of patients, with hypoplasia observed in 1%. These results are consistent with those of Dawoud et al. [25] and Jallu et al. [31]

Conclusion:

Both CT and MRI are essential tools in the preoperative evaluation of CI candidates, as they provide detailed visualization of cochlear development. However, MRI is considered safer for CI candidates, particularly younger patients, as it eliminates the risks associated with radiation exposure inherent in CT imaging. While MRI

remains superior in assessing the cochlear nerve, including its size and detection of its absence, CT can raise suspicion of cochlear nerve hypoplasia or absence in cases of stenosed IAC. Furthermore, the absence of the cochlear nerve is confirmed in individuals with an absent IAC, which can be reliably identified through CT imaging.

Financial support and sponsorship: Nil
Conflict of Interest: Nil

References:

1-Isaacson B. Anatomy and Surgical Approach of the Ear and Temporal Bone. Head Neck Pathol. 2018;12(3):321-327. doi: 10.1007/s12105-018-0926-2

2-Touska P, Connor SEJ. Imaging of the temporal bone. Clin Radiol. 2020;75(9):658-674. doi: 10.1016/j.crad.2020.06.013

3-Alenzi S, Dhanasingh A, Alanazi H, Alsanosi A, Hagr A. Diagnostic Value of 3D Segmentation in Understanding the Anatomy of Human Inner Ear Including Malformation Types. Ear Nose Throat J. 2021;100(5_suppl):675S-683S. doi: 10.1177/0145561320906621

4- Yang SH, Park H, Yoo DS, Joo W, Rhoton A. Microsurgical anatomy of the facial nerve. Clin Anat. 2021;34(1):90-102. doi: 10.1002/ca.23652.

5- Sennaroğlu L, Tahir E. A Novel Classification: Anomalous Routes of the Facial Nerve in Relation to Inner Ear Malformations. Laryngoscope. 2020;130(11):E696-E703. doi: 10.1002/lary.28596

6- Swain SK. Cochlear deformities and its implication in cochlear implantation: a review. Int J Res Med Sci. Int J Res Med Sci. 2022;10(10):2339-2345. doi.org/10.18203/2320-6012.ijrms20222547

7- Costa JR, Coutinho MB, Soares T, Sousa CA e. Bilateral congenital semicircular canal malformation and hearing loss - case report. Nascer e Crescer Growth Med J. 2020;29(1):36-42. https://revistas.rcaap.pt/nascercrescer/article/view/15336

8- Feraco P, Piccinini S, Gagliardo C. Imaging of inner ear malformations: a primer for radiologists. Radiol Med. 2021;126(10):1282-1295. doi: 10.1007/s11547-021-01387-z.

9- Deveze A, Matsuda H, Elziere M, Ikezono T. Diagnosis and Treatment of Perilymphatic Fistula. Adv Otorhinolaryngol. 2018;81:133-145. doi: 10.1159/000485579.

10- Deep NL, Dowling EM, Jethanamest D, Carlson ML. Cochlear Implantation: An Overview. J Neurol Surg B Skull Base. 2019;80(2):169-177. doi: 10.1055/s-0038-1669411.

11- Jain S, Gaurkar S, Deshmukh PT, Khatri M, Kalambe S, Lakhotia P, Chandravanshi D, Disawal A. Applied anatomy of round window and adjacent structures of tympanum related to cochlear implantation. Braz J Otorhinolaryngol. 2019;85(4):435-446. doi: 10.1016/j.bjorl.2018.03.009.

12- Driver EC, Kelley MW. Development of the cochlea. Development. 2020;147(12):dev162263. doi: 10.1242/dev.162263.

13- Spiegel JL, Polterauer D, Hempel JM, Canis M, Spiro JE, Müller J. Variation of the cochlear anatomy and cochlea duct length: analysis with a new tablet-based software. Eur Arch Otorhinolaryngol. 2022;279(4):1851-1861. doi: 10.1007/s00405-021-06889-0.

14- Dawood Y, Strijkers GJ, Limpens J, Oostra RJ, de Bakker BS. Novel imaging techniques to study postmortem human fetal anatomy: a systematic review on microfocus-CT and ultra-high-field MRI. Eur Radiol. 2020;30(4):2280-2292. doi: 10.1007/s00330-019-06543-8.

15- Digge P, Solanki RN, Shah DC, Vishwakarma R, Kumar S. Imaging Modality of Choice for Pre-Operative Cochlear Imaging: HRCT vs. MRI Temporal Bone. J Clin Diagn Res. 2016;10(10):TC01-TC04. doi: 10.7860/JCDR/2016/18033.8592.

16- Ding AS, Lu A, Li Z, Galaiya D, Siewerdsen JH, Taylor RH, Creighton FX. Automated Registration-Based Temporal Bone Computed Tomography Segmentation for Applications in Neurotologic Surgery. Otolaryngol Head Neck Surg. 2022;167(1):133-140. doi: 10.1177/01945998211044982.

17- Singh R, Bhalla AS, Manchanda S, Roychoudhury A. Multidetector computed tomography in preoperative planning for temporomandibular joint ankylosis: A pictorial review and proposed structured reporting format. Imaging Sci Dent. 2021;51(3):313-321. doi: 10.5624/isd.20210027.

18- Sennaroglu L, Ozbal Batuk M. Incomplete Partition Type I. Inner Ear Malformations: Classification, Evaluation and Treatment: Springer; 2022. p. 241-56.

19- Juliano AF. Cross Sectional Imaging of the Ear and Temporal Bone. Head Neck Pathol. 2018;12(3):302-320. doi: 10.1007/s12105-018-0901-y.

20- Brown TH. Childhood hearing impairment. J Paediatr Child Health. 2020;30:6-13. https://doi.org/10.1016/j.paed.2019.10.002

21- Varadarajan VV, Sydlowski SA, Li MM, Anne S, Adunka OF. Evolving Criteria for Adult and Pediatric Cochlear Implantation. Ear Nose Throat J. 2021;100(1):31-37. doi: 10.1177/0145561320947258.

22- Walker N, Pham N, Ledbetter L. Cochlear implantation: Current and future roles of imaging before, during, and after implantation. Curr Radiol Rep. 2023;11:97-107. DOI: 10.1007/s40134-023-00414-3

23- Connor SEJ, Dudau C, Pai I, Gaganasiou M. Is CT or MRI the optimal imaging investigation for the diagnosis of large vestibular aqueduct syndrome and large endolymphatic sac anomaly? Eur Arch Otorhinolaryngol. 2019;276(3):693-702. doi: 10.1007/ s00405-019-05279-x.

24- Parry DA, Booth T, Roland PS. Advantages of magnetic resonance imaging over computed tomography in preoperative evaluation of pediatric cochlear implant candidates. Otol Neurotol. 2005;26(5):976-82. doi: 10.1097/01.mao. 0000185049. 61770 .da.

25- Dawoud MM, Aya M, Mohamad FS, Mohamad HH. Combined diagnostic value of both CT and MRI in pre-operative evaluation of cochlear implant patients. Med J Cairo Univ. 2019;87(5):3289-96. doi: 10.21608/mjcu.2019.65623

26- Wu WJ, He XB, Tan LH, Hu P, Peng AQ, Xiao ZA, Yang S, Wang T, Qing J, Chen X, Li JK, Peng T, Dong YP, Liu XZ, Xie DH. Imaging assessment of profound sensorineural deafness with inner ear anatomical abnormalities. J Otol. 2015;10(1):29-38. doi: 10.1016/j.joto.2015.07.005.

27- Keidar E, Singh J, Santiago-Rivera OJ, Wilkerson B, Babu S. Utility and value of pre-operative CT and MRI for cochlear implantation in the elderly. Am J Otolaryngol. 2021;42(3):102853. doi: 10.1016/j.amjoto.2020.102853.

28- Swarup A, Karakkandy V, Chappity P, Naik S, Behera SK, Parida PK, Grover M, Gupta G, Giri PP, Sarkar S, Pradhan P, Samal DK, Kallyadan Veetil A, Adhikari A, Nayak S. Comparing accuracy of cochlear measurements on magnetic resonance imaging and computed tomography: A step towards radiation-free cochlear implantation. J Otol. 2023;18(4):208-213. doi: 10.1016/j.joto.2023.08.001.

29- Tiwari P, Kumar S, Mishra P, Jain R, Mohindra N, Gupta A, et al. Role of high-resolution CT and MRI in predicting the degree of difficulty in patients undergoing cochlear implant surgery: An institutional experience. Ann Otol Neurotol. 2020;3:1-9. DOI: 10.1055/s-0040-1715552

30- Abd Alla A, Lebda I, Mohamed S, Merwad E. MRI and high resolution CT in congenital hearing loss. Zagazig Univ Med J. 2014;20:1-14. doi: 10.21608/zumj.2014.4357

31- Jallu AS, Jehangir M, Ul Hamid W, Pampori RA. Imaging Evaluation of Pediatric Sensorineural Hearing Loss in Potential Candidates for Cochlear Implantation. Indian J Otolaryngol Head Neck Surg. 2015;67(4):341-6. doi: 10.1007/s12070-015-0819-6.